Toward Understanding the Effect of Water Sorption on Lithium Zirconate (Li_2ZrO_3) during Its Carbonation Process at Low Temperatures

Lorena Martínez-dlCruz and Heriberto Pfeiffer*

Instituto de Investigaciones en Materiales, Universidad Nacional Autónoma de México, Circuito exterior s/n, Ciudad Universitaria, Del. Coyoacán, CP 04510, México DF, MEXICO

Received: March 8, 2010; Revised Manuscript Received: April 16, 2010

Lithium metazirconate with and without potassium were synthesized by solid-state reaction. Different water vapor sorption experiments were performed in the presence and absence of CO_2 to elucidate the different physicochemical processes produced. In the absence of CO_2, initial results showed that potassium addition enhances significantly the water sorption on the Li_2ZrO_3 ceramic. Then, it was shown that water vapor is trapped by two different mechanisms on Li_2ZrO_3, adsorption and absorption. When CO_2 was added to water vapor flow the Li_2ZrO_3 reactivity increased significantly. On the basis of these results, a possible $K-Li_2ZrO_3-H_2O-CO_2$ reaction mechanism was proposed; as a first step Li_2ZrO_3 and H_2O must react producing some Li−OH and Zr−OH species. Then, CO_2 must react with hydroxyl species (mainly Li−OH), producing lithium carbonate. Finally, the presence of this new specie must favor a higher water adsorption.

Introduction

Several lithium ceramics have been widely studied as tritium breeding materials for nuclear fusion reactor, as electronic devices, and in low thermal expansion glass ceramics used in ceramic hobs.[1−5] Additionally, in recent years, these ceramics have been proposed as promising carbon dioxide (CO_2) captors as well.[6−11]

In all these technological applications, as in others, the exposition of lithium ceramics to water vapor may affect its performance. For example, the hygroscopic nature of lithium ceramics is a critical factor on the materials selection for the design and fabrication of ceramics breeders, due to their moisture affinity, which can produce a decrement on its properties by the presence of adsorbed water.[12] Another specific example is the use of lithium ceramics as CO_2 captors, for example, lithium metazirconate (Li_2ZrO_3) or lithium orthosilicate (Li_4SiO_4).[6,13−18] In fact, in a real CO_2 capture system, since water vapor is a combustion product, then solids absorbents would be exposed to wet environments, especially if postcombustion capture technologies were used.[19] In this sense, some papers have shown that exposition of these solid absorbents to wet environments can affect the CO_2 sorption performance.[9,20,21] Nevertheless, these works do not necessary agree among them. For example, while Essaki et al.[20] and Ochoa-Fernández et al.[21] showed that water vapor improves the CO_2 absorption on lithium and sodium ceramics, some results presented by Nair et al.[9] suggested that water presence on some lithium ceramics inhibits the CO_2 absorption.

Therefore, as the mechanism involving the reaction between lithium ceramics and H_2O vapor seems to modify the CO_2 absorption but is still uncertain, the aim of this work was to study systematically the different physicochemical phenomena present during the hydration process of Li_2ZrO_3 in the presence and absence of CO_2. Li_2ZrO_3 was chosen as an initial case of study, as this material is one of the most studied ceramics into the CO_2 absorption field.

* To whom correspondence should be addressed. Phone +52(55)56224627. Fax +52(55)56161371. E-mail pfeiffer@iim.unam.mx.

Experimental Procedure

Pure lithium zirconate (Li_2ZrO_3) and potassium-doped lithium zirconate ($K-Li_2ZrO_3$) were synthesized by solid-state reaction. $K-Li_2ZrO_3$ was synthesized, as it has been reported that potassium addition importantly improves the CO_2 absorption on this ceramic.[13−15] Then, the reagents used were zirconium oxide (ZrO_2, Aldrich), lithium carbonate (Li_2CO_3, Aldrich) and potassium carbonate (K_2CO_3, Aldrich), where the Li_2CO_3/ZrO_2 and $Li_2CO_3/ZrO_2/K_2CO_3$ molar ratios were 1.1:1.0 and 1.1:1.0:0.1, respectively. Ceramics were prepared by solid-state reaction, where the corresponding amounts of the different reagents were mechanically mixed and then fired at 850 °C for 12 h. The correct composition and structure of the Li_2ZrO_3 materials were confirmed by XRD (data not shown), which confirmed the synthesis of the monoclinic Li_2ZrO_3 phase in both cases. Additionally, the surface area of the samples was determined by N_2 adsorption using the BET model.[22,23] The equipment used in this case was a Minisorp II from Bel-Japan at 77 K using a multipoint technique. Samples were previously activated at 85 °C for 20 h in vacuum.

For water sorption analyses, different dynamic experiments were carried out on a temperature-controlled thermobalance Q5000SA from TA Instruments, equipped with a humidity-controlled chamber. The experimental variables were temperature, time, and relative humidity (RH). The experiments were carried out using N_2 or CO_2, both Praxair (grade 4.8 and 4.0, respectively), as carrier gases and distilled water as the vapor precursor, using in all the cases a total gas flow of 100 mL/min. The RH percentages were controlled automatically with the Q5000SA equipment. First, different water vapor sorption/desorption isotherms were generated varying temperature, between 30 and 80 °C, from 0 to 80 to 0% of RH. Then, another set of experiments was performed but in this case fixing the RH and varying temperature from 30 to 80 °C.

After water sorption experiments and to identify the hydration products, powders after the hydration processes were characterized by standard thermogravimetric (TGA) and infrared (FTIR) analyses. For the TG analyses, the experiments were performed under air atmosphere with a heating rate of 5 °C/min into a

10.1021/jp1020966
Published on Web 05/03/2010

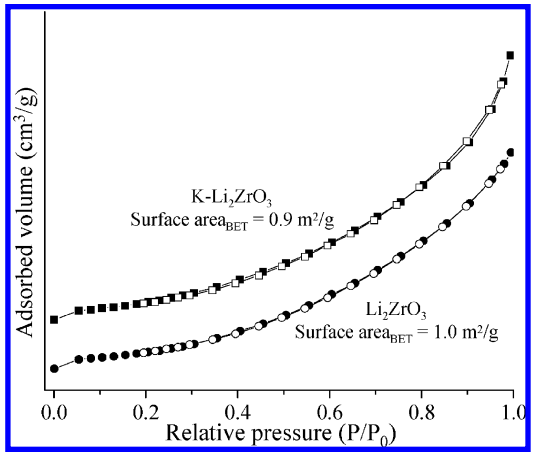

Figure 1. N_2 adsorption/desorption isotherms of the Li_2ZrO_3 and K−Li_2ZrO_3 samples.

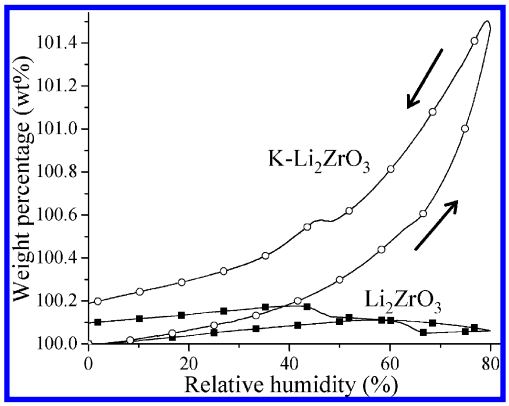

Figure 2. Water sorption/desorption isotherms of the Li_2ZrO_3 and K−Li_2ZrO_3 samples, generated at 80 °C, using N_2 as carrier gas.

thermobalance TA Instruments model Q500HR. For the FTIR spectroscopy, samples were prepared as KBr pellets. Then, analyses were performed on a Spectrometer NICOLET 6700 FT-IR.

Results and Discussion

Initially, the external surface area of the Li_2ZrO_3 and K−Li_2ZrO_3 samples was determined. The N_2 adsorption/desorption isotherms are shown in Figure 1. Both samples presented very similar isotherms, and according to the IUPAC classification both presented isotherm curves of type II.[23] This kind of isotherms are typically obtained in nonporous adsorbents, where unrestricted monolayer−multilayer adsorption processes can occur. This result is in good agreement with the synthesis method used, solid-state reaction. Then, surface area was determined using the BET model, obtaining the following results: 1.0 and 0.9 m^2/g for the Li_2ZrO_3 and K−Li_2ZrO_3 samples, respectively. It shows that potassium addition did not importantly modify the surface area of the samples.

Then, water vapor sorption/desorption isotherms were performed using N_2 as carrier gas, in both samples. N_2 was initially used, as an inert gas, to elucidate exclusively the H_2O water effect over the ceramic particles. The results presented very important differences between the samples (Figure 2). While the K−Li_2ZrO_3 sample depicted a well-defined water sorption/desorption process, Li_2ZrO_3 practically did not trap water. As the external surface area of both samples was very similar, this behavior may be explained exclusively in terms of the high hydrophilic properties of potassium in comparison to lithium.

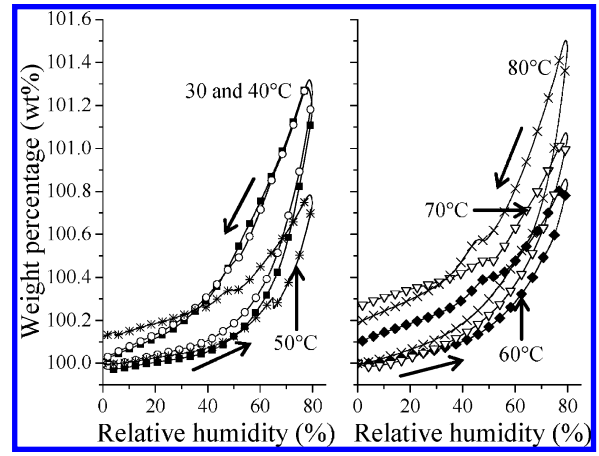

Figure 3. Water sorption/desorption isotherms of the K−Li_2ZrO_3 sample, generated at different temperatures (30, 40, 50, 60, 70, and 80 °C), using N_2 as carrier gas.

Therefore, all the following analyses were only performed on the K−Li_2ZrO_3 sample, as this sample was the only one that presented interesting water sorption properties.

Figure 3 shows different water vapor sorption/desorption isotherms for the K−Li_2ZrO_3 sample, varying temperature. In these cases and according to the IUPAC classification, all the water sorption isotherms presented curves of type III.[23] In fact, these isotherms are commonly obtained in systems where the interactions between the adsorbate and the adsorbent are considerably weak, in comparison to the adsorbate−adsorbate interactions. Besides, although all the isotherms presented hysteresis loops, two different behaviors were observed. At 30 and 40 °C, the hysteresis loops close and this behavior suggest that water sorption/desorption processes are totally reversible. In addition, the maximum increment of weight at 80% of RH was almost the same (1.3 wt %) for both thermal conditions (Figure 3A). Then, it should be assumed that the observed process was water adsorption over the K−Li_2ZrO_3 surface, and in these cases the weight gained by the samples was only due to the increasing thickness of multilayer water adsorbed films. On the other hand, for the samples treated at 50 °C or higher temperatures the hysteresis loops did not close. Here, samples presented a final weight gain after desorption process. These results suggest that not only a water adsorption was carried out, but a chemical process could have occurred as well. It would be attributed to a hydroxylation process over the K−Li_2ZrO_3 surface.

A more detailed analysis of the sorption/desorption isotherms shows that samples trapped different quantities of water as a function of the temperature. Between 30 and 40 °C, samples practically did not show any kind of variation when the RH was increased up to 80%. Then, when the temperature was increased to 50 °C the tendency of water molecules to be trapped became less pronounced at the highest RH percentage (80%) although the final adsorption after the desorption process was higher. This suggests a weaker water condensation, which may be attributed to an increment of the evaporation rate due to temperature. Conversely, sorption isotherms performed at 60, 70, and 80 °C did not follow this trend. In those cases, the water trapped increased again, as a function of temperature. This behavior has to be explained by the presence of different processes at the following specific conditions: as the sorption/desorption curves did not close, it was previously suggested that not only water adsorption went through, but a chemical reaction took place, so an absorption process happened.

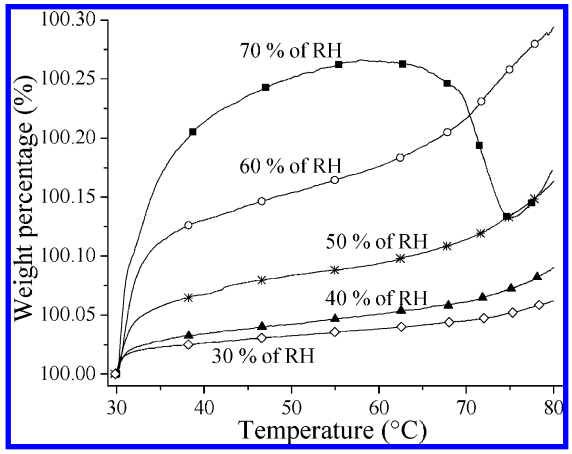

Figure 4. Thermal dynamic curves of water sorbed on $K-Li_2ZrO_3$, varying the relative humidity (30, 40, 50, 60, and 70% of RH), using N_2 as carrier gas.

However, the water absorbed may not completely explain the total weight gain during the RH increment. Nevertheless, a chemical surface modification may favor a larger water adsorption, even at higher temperatures.

Additionally, it should be mentioned that most of the isotherms presented two different loss of weight during desorption or dehydration stage. The first one was presented between 77 and 48% RH, while the second one began at around 43% RH. The first lost of weight can be explained as spontaneous evaporation of condensed water located at the particle surfaces, and the second process must correspond to evaporation of water located at interparticle spaces. So, when the equilibrium between adsorbed film and saturated vapor atmosphere in the system change and the adsorption process became reversible.

A second set of $K-Li_2ZrO_3$ samples was evaluated fixing the RH and increasing temperature at 1 °C/min (Figure 4). In these cases, most of the curves presented the same behavior. Initially, as soon as the RH was established all the curves presented a gain of weight, which should be attributed to water adsorption. Of course, the quantity of adsorbed water increased as a function of the RH, as it could be expected, from 0.022 to 0.11 wt % for samples treated at 30 and 70% of RH, respectively. After this initial process, samples presented two different increments of weight, which should be attributed to a mixture of water adsorption and absorption. These two processes occurred between 32 and 55 °C in the first case and at temperatures equal or higher than 60 °C in the second case. The first process may be mainly attributed to the water adsorption, while the second one must correspond basically to a chemical reaction between water and the $K-Li_2ZrO_3$ surface. The double process is proposed because if water were only adsorbed, higher temperatures must propitiate a decrement of weight through water evaporation. Instead, as the weight increased even at high temperatures, the water reaction is more plausible when temperature increases. In fact, a sample treated with 70% of RH is an extreme case, which qualitatively confirms this hypothesis. In this case, the thermogram presents initially an exponential increment of weight up to 62−63 °C. This increment of weight should be attributed to a mixture of adsorbed and absorbed water. Then, between 63 and 75 °C, it can be observed an abrupt lost of weight of around 50% of the total weight previously gained. This process must correspond to the evaporation of adsorbed water. Note that around 50 wt % of the initial weight gained corresponds to adsorbed water. Finally, the thermogram continued showing an increment of

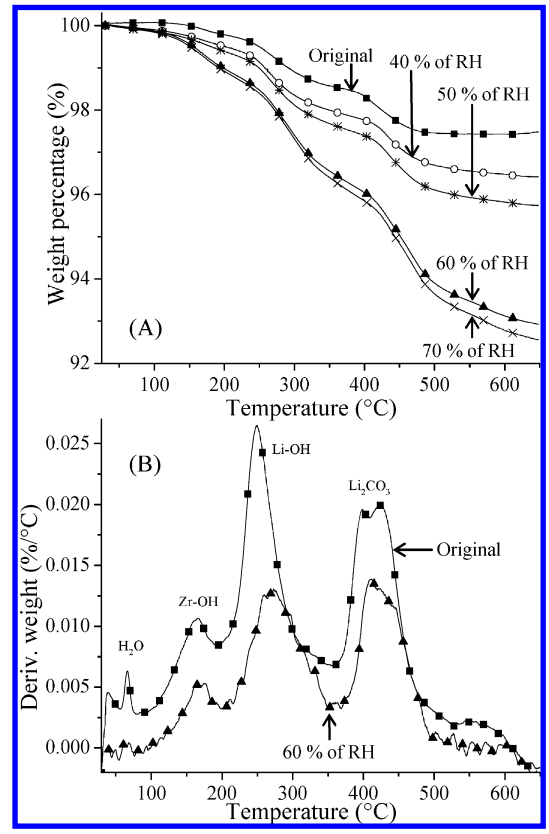

Figure 5. TGA (A) and DTGA (B) curves of the $K-Li_2ZrO_3$ samples after different humidity treatments performed at 60 °C.

weight as a function of temperature, which must correspond to water absorption.

To analyze the hydration products obtained during the H_2O sorption processes, the $K-Li_2ZrO_3$ sample was isothermically treated at different temperatures and RH. Then, products were analyzed using TGA and FTIR.

Different samples previously thermal-humidity treated, as well as the $K-Li_2ZrO_3$ original sample, were analyzed by TGA. Figure 5 shows the thermograms of samples thermal-humidity treated at 60 °C and RH of 40, 50, 60, and 70% and the original $K-Li_2ZrO_3$ ceramic. It is evident that although all samples presented a similar trend, the thermal-humidity conditions in which each sample was tested during the H_2O isothermal experiments modified the weight loss in each thermal step (Figure 5A). Initially, while the original sample did not lose weight between room temperature and 100 °C, all the other samples lost around 0.15−0.2 wt %, which is merely adsorbed water. Then, between 100 and 215 °C, each sample lost different weights, which in this case should be attributed to a Zr−OH dehydroxylation process.[24,25] The quantity of weight lost for each sample was 0.3, 0.6, 0.8, 1.3, and 1.4 wt % for the original sample and samples treated 40, 50, 60, and 70% of RH. When the temperature was increased from 235 to 350 °C, the samples presented a third loss of weight. The weight loss produced at these temperatures could be attributed to a second dehydroxylation process, in this case due to the Li−OH species produced during the water reaction with the ceramic.[26,27] It should be mentioned that according to the weight lost in these two thermal processes, lithium hydroxylation seems to be favored over the zirconium hydroxylation. Finally, a decarbonation process was observed at temperatures higher than 400 °C. Part of the carbonates were present since the beginning of the experiments, as it can be seen in the original sample, and the rest of them

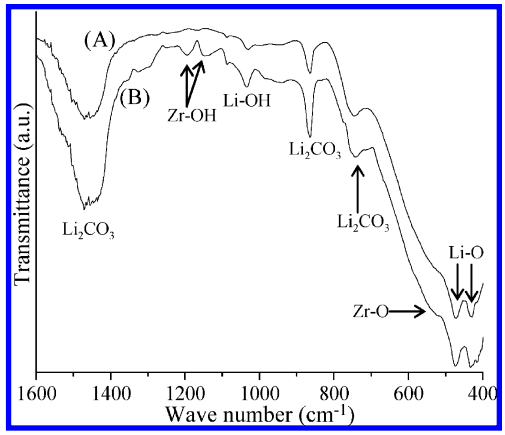

Figure 6. Infrared spectra of the K−Li_2ZrO_3 sample after different thermal-humidity treatments: (A) K−Li_2ZrO_3 original sample (without any treatment) and (B) K−Li_2ZrO_3 sample heat treated at 70 °C with 70% of RH.

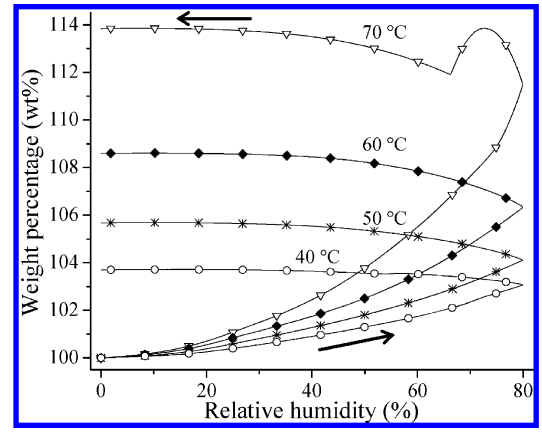

Figure 7. Water sorption/desorption isotherms of the K−Li_2ZrO_3 sample, generated at different temperatures (40, 50, 60, and 70 °C), using CO_2 as carrier gas.

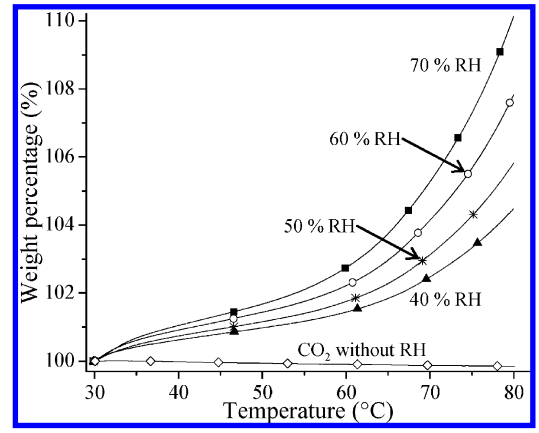

Figure 8. Thermal dynamic curves of water and CO_2 sorbed on K−Li_2ZrO_3, varying the relative humidity (40, 50, 60, and 70% of RH), using CO_2 as carrier gas. The curve labeled as CO_2 without RH corresponds to a sample heat treated into a dry CO_2 flow.

should be trapped after the water sorption process, from the environment. It is evident that the weight loss varied as a function of the hydroxyl and carbonate groups formed, as follows $Li_2ZrO_3^{70\%RH}$ > $Li_2ZrO_3^{60\%RH}$ > $Li_2ZrO_3^{50\%RH}$ > $Li_2ZrO_3^{40\%RH}$ > $Li_2ZrO_3^{original}$. It implies that even Li_2ZrO_3 without any thermal-humidity treatment already possessed some hydroxyl and carbonate groups over the surface of the particles, which must be produced due to the contact of these particles with the atmosphere. Additionally, from the derivate curves (Figure 5B), it seems that average temperatures for all the processes are slightly shifted to higher temperatures, which may be simply attributed to kinetic factors due to the presence of higher quantities of the different species. Something else has to be pointed out from these thermograms. This sample contains potassium, which should have contributed to the hydroxylation and carbonation processes detected by TGA, as it was evidenced and discussed previously in Figure 2. However, as the potassium content is very low, it was not possible to detect and differentiate these specific thermal signals.

FTIR spectra (Figure 6) showed the presence of different absorption bands characteristic of zirconium−oxygen and lithium−oxygen bonds, as well as carbonate and hydroxyl species located over the surface of the particles. The FTIR analysis was performed over different samples treated isothermically 70 °C, varying the RH. In general, K−Li_2ZrO_3 sample, before and after the thermal-humidity treatments, presented similar FTIR spectra. Initially, between 400 and 600 cm^{-1}, the three different bands presented correspond to structural Li−O (431 and 476 cm^{-1}) and Zr−O (530 cm^{-1}) vibrations.[28,29] Then, Li_2CO_3 produced bands at 730, 860, and 1443 cm^{-1}.[28,30] As mentioned previously, lithium carbonate was produced by the sample contact with the environment, before and after the thermal-humidity treatments. Finally the presence of superficial bending modes of Li−OH (1035 cm^{-1}) and Zr−OH (1146 and 1197 cm^{-1}) bands were elucidated between 1000 and 1200 cm^{-1}.[31] It should be noted that Zr−OH bands grew after the thermal-humidity treatments, suggesting that temperature induces its formation. Therefore, the FTIR and TGA results confirmed the presence of hydroxyl and carbonate species over the K−Li_2ZrO_3 surface, which were produced after the thermal-humidity treatments.

After the water sorption analysis performed on K−Li_2ZrO_3, using N_2 as carrier gas, similar experiments were performed on this sample, but now using CO_2 as carrier gas. The water sorption/desorption isotherms are presented in figure 7. As in the N_2 cases, sorption curves presented isotherms of type III.[23] However, the weight variations, using CO_2, were much larger than those observed using N_2 (see figure 3). The total weight gained, in any thermal and RH conditions were always at least 1 order of magnitude larger with the CO_2 flow. Additionally, the total weight gained increased as a function of temperature. Finally, in these cases, hysteresis loops did not closed in the curves. From these results it must be assumed that K−Li_2ZrO_3 surface reactivity has been importantly increased with the CO_2 addition.

Again, as in the N_2 case, a second set of K−Li_2ZrO_3 samples were evaluated fixing the RH and increasing temperature at 1 °C/min, using CO_2 as carrier gas (Figure 8). All the curves, containing CO_2 and water vapor, presented similar behaviors. Initially, as soon as the RH was established all the curves presented the gain of weight, which was attributed to water adsorption. The quantity of water adsorbed increased as a function of the RH, as it could be expected, from 0.4 to 0.7 wt % for samples treated at 40 and 70% of RH, respectively. After this initial process, samples presented a constant increment of weight as a function of temperature, and the final quantity of weight gained increased as a function of the RH. Although it is well-known that K−Li_2ZrO_3 is only able to trap CO_2 at temperatures higher than 400 °C,[13−15] the final curve presents the case where CO_2 was used without the presence of H_2O. As it can be seen, under these conditions the weight gained was negligible, in comparison to the samples treated with H_2O. From

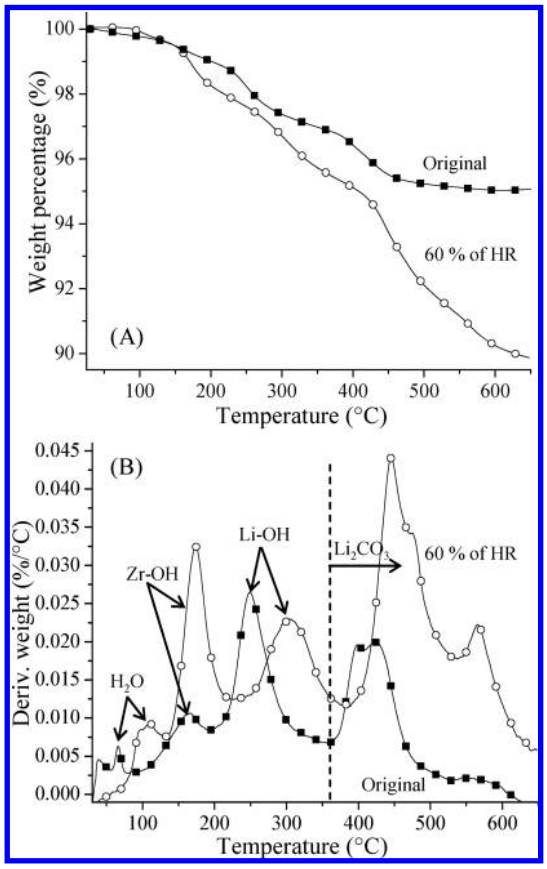

Figure 9. TGA (A) and DTGA (B) curves of the K−Li_2ZrO_3 original and thermal-humidity treated (T = 60 °C and RH = 60%, using CO_2 as carrier gas) samples.

all these experiments, perhaps, the most important results is the fact that CO_2 presence as carrier gas produced a very important increment on the total weight gained in comparison to the same experiments performed with N_2. The observed differences must be mainly attributed to the following double step reaction system: (1) water absorption and (2) CO_2 reactivity with the hydroxylated surfaces.

Of course, To corroborate the mechanism proposed, samples were characterized after the thermal-hydration processes. Figure 9 shows the TG and DTG results obtained for the sample treated with 60% of RH and CO_2 in comparison with the original sample. As in the samples treated with N_2, thermograms presented similar trends, producing mass changes due to dehydration, dehydroxylation (Zr−OH and Li−OH) and decarbonation processes. However, as it could be expected, the total weight lost on the CO_2 treated sample (10.2 wt %) was twice larger than the original sample (4.6 wt %). Additionally, from the DTG analyses, it can be seen that all the processes were shifted to higher temperatures when sample was treated with CO_2, even the evaporation process. To explain this behavior it has to be considered that on the initial sample all the processes were mainly produced over the surface of the K−Li_2ZrO_3 particle. On the other hand, sample treated with CO_2 and water vapor produced much larger quantities of products (Zr−OH species, Li−OH, and Li_2CO_3), which may imply intra- and interparticle diffusion effects. Furthermore, according to the DTG curves, the increment of the Zr−OH species seems to be larger than the increment of the Li−OH species, and the carbonate species increased as well importantly. On the basis of these results and the fact that K−Li_2ZrO_3 is not able to trap CO_2 at these temperatures without the presence of water vapor, it would be possible to propose a K−Li_2ZrO_3−H_2O−CO_2 reaction mechanism. Initially, K−Li_2ZrO_3 and H_2O must react producing some Li−OH and Zr−OH species at the surface of the K−Li_2ZrO_3 particles. Then, CO_2 must react with the hydroxyl species (mainly the lithium ones according to the DTG results), producing lithium carbonate. Finally, the presence of this new specie must favor a higher water adsorption.

Conclusions

Initially, it was observed that potassium addition on the Li_2ZrO_3 sample modified importantly the water sorption characteristics, becoming more hygroscopic. Additionally, the experiments performed using N_2 as carrier gas clearly showed that K−Li_2ZrO_3 is able to trap water by two different mechanisms, adsorption and absorption. The generation of any of these sorption processes depends on different factors such as temperature and relative humidity concentration. Therefore, the stability and/or chemical reactivity of K−Li_2ZrO_3 ceramics is altered by the presence of water.

Later, when CO_2 was used as carrier gas, the K−Li_2ZrO_3 sample continued trapping water by the same two mechanisms, adsorption and absorption. Nevertheless, under these new conditions CO_2 was chemically trapped as carbonates. Furthermore, the total weight gained under these conditions was 10 times higher than that observed using N_2, where this increment of weight was produced by a hydroxylation increment and by the carbonation appearance.

Finally, according to literature, K−Li_2ZrO_3 is not able to trap CO_2 until 400−450 °C, under dry conditions. Therefore, the presence of water vapor importantly improves the CO_2 absorption, at least on this temperature range (30−80 °C).

Acknowledgment. Lorena Martínez-dlCruz thanks CONACYT for financial support. This work was performed into the IMPULSA-PUNTA framework of the Universidad Nacional Autónoma de México and financially supported by CONACYT (60980, 23148), PAPIIT-UNAM (IN100609), and ICyT-DF (179/2009). Furthermore, authors thank M. A. Canseco-Martínez and E. Fregoso-Israel for technical help.

References and Notes

(1) Lu, C. H.; Wei-Cheng, L. *J. Mater. Chem.* **2000**, *10*, 1403.
(2) Subramanian, V.; Chen, C. L.; Chou, H. S.; Fey, G. T. K. *J. Mater. Chem.* **2001**, *11*, 3348.
(3) Johnson, C. E.; Clemmer, R. G.; Hollenberg, G. W. *J. Nucl. Mater.* **1981**, *103*, 547.
(4) Kopasz, J. P.; Seils, C. A.; Johnson, C. E. *J. Nucl. Mater.* **1994**, *212−215*, 912.
(5) Pfeiffer, H.; Bosch, P.; Bulbulian, S. *J. Nucl. Mater.* **1998**, *257*, 309.
(6) Xiong, R.; Ida, J.; Lin, Y. S. *Chem. Eng. Sci.* **2003**, *58*, 4377.
(7) Kato, M.; Nakagawa, K.; Essaki, K.; Maezawa, Y.; Takeda, S.; Kogo, R.; Hagiwara, Y. *Int. J. Appl. Ceram. Technol* **2005**, *2*, 467.
(8) Alcérreca-Corte, I.; Fregoso-Israel, E.; Pfeiffer, H. *J. Phys. Chem. C* **2008**, *112*, 6520.
(9) Nair, B. N.; Burwood, R. P.; Goh, V. J.; Nakagawa, K.; Yamaguchi, T. *Prog. Mater. Sci.* **2009**, *54*, 511.
(10) Ávalos-Rendón, T.; Casa-Madrid, J.; Pfeiffer, H. *J. Phys. Chem. A* **2009**, *113*, 6919.
(11) Mejía-Trejo, V. L.; Fregoso-Israel, E.; Pfeiffer, H. *Chem. Mater.* **2008**, *20*, 7171.
(12) Roux, N.; Tanaka, S.; Johnson, C.; Verrall, R. *Fusion Eng. Des.* **1998**, *41*, 31.
(13) Ida, J.; Xiong, R.; Lin, Y. S. *Sep. Purif. Technol.* **2004**, *36*, 41.
(14) Ida, J.; Lin, Y. S. *Environ. Sci. Technol.* **2003**, *37*, 1999.
(15) Pannocchia, G.; Puccini, M.; Seggiani, M.; Vitolo, S. *Ind. Eng. Chem. Res.* **2007**, *46*, 6696.
(16) Ochoa-Fernández, E.; Rusten, H. K.; Jakobsen, H. A.; Rønning, M.; Holmen, A.; Chen, D. *Catal. Today* **2005**, *106*, 41.

(17) Ochoa-Fernández, E.; Rønning, M.; Grande, T.; Chen, D. *Chem. Mater.* **2006**, *18*, 1383.
(18) Ochoa-Fernández, E.; Rønning, M.; Yu, X.; Grande, T.; Chen, D. *Ind. Eng. Chem. Res.* **2008**, *47*, 434.
(19) Figueroa, J. D.; Fout, T.; Plasynski, S.; Macllvried, H.; Srivastava, R. D. *Int. J. Greenhouse Gas Control* **2008**, *2*, 9.
(20) Essaki, K.; Nakagawa, K.; Kato, M.; Uemoto, H. *J. Chem. Eng. Jpn.* **2004**, *37*, 772.
(21) Ochoa-Fernández, E.; Zhao, T.; Ronning, M.; Chen, D. *J. Environ. Eng.* **2009**, *37*, 397.
(22) Rouquerol, F.; Rouquerol, J.; Sing, K. *Adsorption by Powders and Porous Solids: Principles, Methodology and Applications*; Academic Press: New York, 1999; p. 97.
(23) McCash, E. M. *Surface Chemistry*; Oxford Press: New York, 2002; p. 72.
(24) Ali, A. A. M.; Kaki, M. I. *Thermochim. Acta* **1999**, *336*, 17.
(25) Ali, A. A. M.; Kaki, M. I. *Colloids Surf., A* **1998**, *139*, 81.
(26) Choi, K. S.; Yeon, J. W.; Park, Y. S.; Ha, Y. K.; Han, S. H.; Song, K. *J. Alloys Comp.* **2009**, *486*, 824.
(27) Veliz-Enriquez, M. Y.; Gonzalez, G.; Pfeiffer, H. *J. Solid State Chem.* **2007**, *180*, 2485.
(28) Zhang, B.; Nieuwoudt, M.; Easteal, A. J. *J. Am. Ceram. Soc.* **2008**, *91*, 1927.
(29) Ravikrishna, R.; Green, R.; Valsaraj, K. T. *J. Sol-Gel Sci. Tech.* **2005**, *34*, 111.
(30) Zhang, D. R.; Liu, H. L.; Jin, R. H.; Zhang, N. Z.; Liu, Y. X.; Kang, Y. S. *J. Ind. Eng. Chem.* **2007**, *13*, 92.
(31) Wilmarth, W. R.; Walker, D. D.; Fondeur, F. F.; Fink, S. D.; Mills, J. T.; Dukes, V. H.; Croy, B. H. WSRC-TR-2001−00221, 2001.

JP1020966